Article

Immunity

Perforin-Positive Dendritic Cells Exhibit an Immunoregulatory Role in Metabolic Syndrome and Autoimmunity

Graphical Abstract

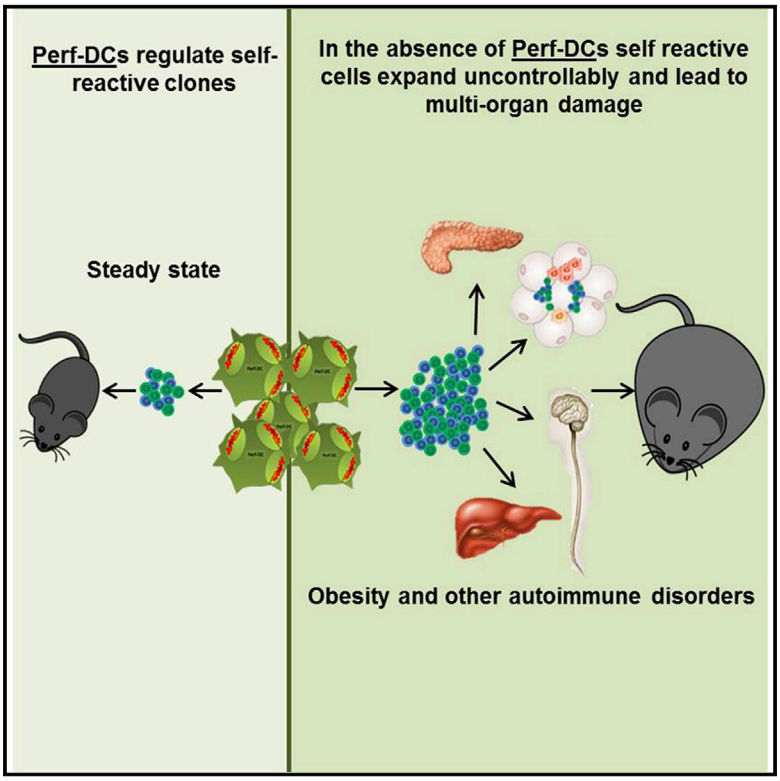

Authors

Yael Zlotnikov-Klionsky, Bar Nathansohn-Levi, Elias Shezen, ..., Oren Yifa, Anna Aronovich, Yair Reisner

Correspondence

yair.reisner@weizmann.ac.il

In Brief

Perforin-positive dendritic cells (perf-DCs) represent a minor subpopulation of myeloid DCs. Based on selective ablation of perf-DCs in radiation chimera, Reisner and colleagues demonstrate that these cells control inflammatory T cells in steady state and play a regulatory role in metabolic syndrome and in experimental autoimmune encephalomyelitis.

Highlights

- Mice lacking perforin$^+$ DCs gain weight and exhibit features of metabolic syndrome
- The onset of this phenotype can be accelerated upon feeding with high-fat diet
- The phenotype can be completely prevented by T cell depletion in vivo
- Similar impact on T cells by perf-DCs was found in a model of multiple sclerosis

Zlotnikov-Klionsky et al., 2015, Immunity *43*, 776–787
October 20, 2015
http://dx.doi.org/10.1016/j.immuni.2015.08.015

CellPress

CellPress

Immunity
Article

Perforin-Positive Dendritic Cells Exhibit an Immuno-regulatory Role in Metabolic Syndrome and Autoimmunity

Yael Zlotnikov-Klionsky,[1,2] Bar Nathansohn-Levi,[1,2] Elias Shezen,[1] Chava Rosen,[1] Sivan Kagan,[1] Liat Bar-On,[1] Steffen Jung,[1] Eric Shifrut,[1] Shlomit Reich-Zeliger,[1] Nir Friedman,[1] Rina Aharoni,[1] Ruth Arnon,[1] Oren Yifa,[1] Anna Aronovich,[1] and Yair Reisner[1,*]

[1]Department of Immunology, Weizmann Institute of Science, Herzel St 1, Rehovot 76100, Israel

[2]Co-first author

*Correspondence: yair.reisner@weizmann.ac.il

http://dx.doi.org/10.1016/j.immuni.2015.08.015

SUMMARY

Emerging evidence suggests that immunological mechanisms underlie metabolic control of adipose tissue. Here, we have shown the regulatory impact of a rare subpopulation of dendritic cells, rich in perforin-containing granules (perf-DCs). Using bone marrow transplantation to generate animals selectively lacking perf-DCs, we found that these chimeras progressively gained weight and exhibited features of metabolic syndrome. This phenotype was associated with an altered repertoire of T cells residing in adipose tissue and could be completely prevented by T cell depletion in vivo. A similar impact of perf-DCs on inflammatory T cells was also found in a well-defined model of multiple sclerosis, experimental autoimmune encephlalomyelitis (EAE). Thus, perf-DCs probably represent a regulatory cell subpopulation critical for protection from metabolic syndrome and autoimmunity.

INTRODUCTION

Studies of cellular mechanisms involved in maintenance of peripheral immune tolerance have largely focused on T regulatory (Treg) cells, but other key cellular mediators such as B regulatory (B reg) cells, myeloid suppressor cells (MDSCs), and various types of dendritic cells (DCs) have been implicated, as well. DCs have a tolerogenic capacity in their immature state (Dhodapkar et al., 2001; Fu et al., 1996; Jonuleit et al., 2000; Lutz et al., 2000; Tiao et al., 2005; Trinité et al., 2005). However, this rather simplistic dichotomy between mature and immature DCs has been challenged by the demonstration that fully mature DCs can also induce tolerance under appropriate conditions (Lu et al., 1997; Süss and Shortman, 1996; Waithman et al., 2007; Yu et al., 2009).

We have recently described the generation of a highly defined population of DCs from $Lin^{-}Sca1^{+}cKit^{+}$ (LSK) hematopoietic progenitors (Zangi et al., 2012). These DCs express perforin and granzyme A in discrete granules and are therefore termed "perf-DCs" (Zangi et al., 2012). Perf-DCs are able to selectively kill cognate T cell receptor (TCR) transgenic $CD8^{+}$ T cells that recognize their peptide-MHC, through a unique perforin and granzyme A-based killing mechanism, regulated through toll-like receptor-7 (TLR7) and triggering receptor expressed on myeloid cells-1 (TREM-1) signaling (Zangi et al., 2012). We demonstrated by immune histological staining that perf-DCs comprise about 2%–4% of the CD11c-positive cells within the lymph nodes and spleen and that the abundance of these cells is markedly enhanced upon in vivo administration of granulocyte macrophage colony stimulating factor (GM-CSF) (Zangi et al., 2012).

Perforin-positive myeloid DCs have also been reported within the human classical DC population (Stary et al., 2007). These initial findings, based exclusively on ex vivo studies, indicated a potential tolerogenic role for perf-DCs; however, the relevance of this cell population to tolerance maintenance in the steady state in vivo remained unresolved.

To address this question, we used bone marrow transplantation to generate chimeric mice, in which perforin expression is selectively impaired in CD11c-positive DCs. We found that, within 5 months, these mice developed many features of metabolic syndrome, suggesting that perf-DCs represent an important regulatory population that might control inflammatory processes in the adipose tissue (AT). Our results are in line with the emerging intriguing cross-talk between the immune system and the endocrine AT (Hotamisligil et al., 1993; Weisberg et al., 2003; Xu et al., 2003). Specifically, these studies suggest that AT dysfunction and metabolic imbalances in obesity are associated with low-grade systemic inflammation.

The antigens that drive AT-specific T cell selection and expansion resulting in the observed AT inflammation are not yet known. We therefore investigated the regulatory role of perf-DCs in a more defined model of autoimmunity, namely experimental autoimmune encephalomyelitis (EAE). In line with our hypothesis that perf-DCs have immuno-regulatory activity, mice lacking these cells were substantially more prone to induction of EAE, exhibiting significantly elevated autoimmune T cell clones compared to their WT counterparts. Collectively, we demonstrate that perf-DCs mediate a key role in steady-state protection from development of metabolic syndrome, as well as in the control of EAE.

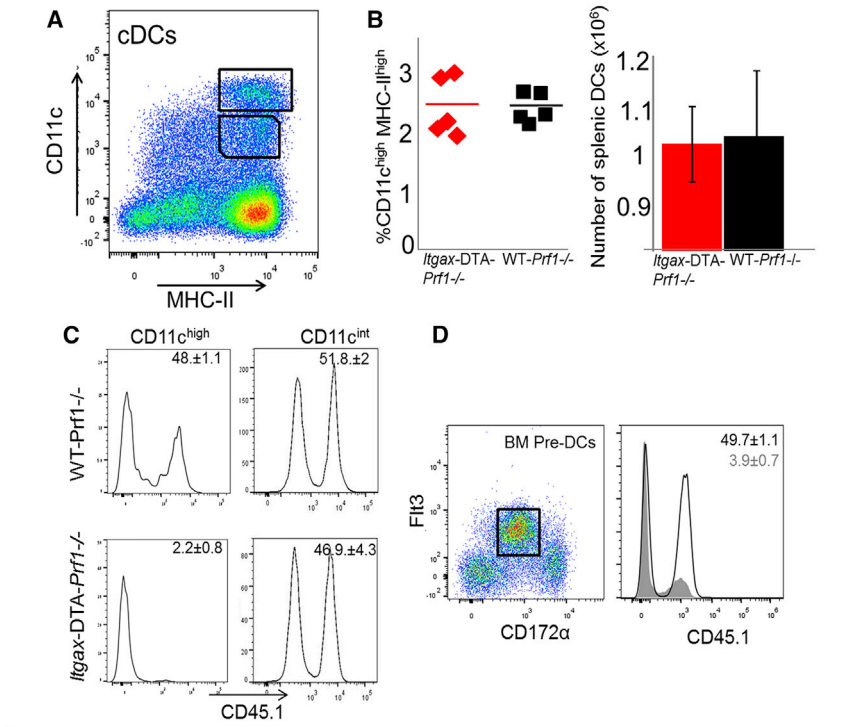

Figure 1. Characterization of Donor Type Origin in Immune Cells of WT-*Prf1*$^{-/-}$ and *Itgax*-DTA-*Prf1*$^{-/-}$ Chimeras

(A) Flow cytometry analysis of CD11c^{+} cells from spleen of *Itgax*-DTA-*Prf1*$^{-/-}$ chimeric mice and WT-*Prf1*$^{-/-}$ controls. The CD11c^{+} cells could be divided into CD11c^{hi} (cDCs) and CD11c^{int} subpopulations.

(B) cDC expression in the spleen of *Itgax*-DTA-*Prf1*$^{-/-}$ and WT-*Prf1*$^{-/-}$ chimeras. Error bars represent mean ± SD.

(C) The cells defined in (A) were further stained for CD45.1 to identify cell origin from *Itgax*-DTA mice or littermate controls, or for CD45.2 expressed by *Prf1*$^{-/-}$ donors. Numbers indicate percent of CD45.1 cells in the various populations (mean ± SD, n ≥ 5).

(D and E) Donor origin as defined by flow cytometry analysis of CD45.1 and CD45.2 of BM pre-DCs (D), B cells, NK cells, pDCs, T cells, and neutrophils (E) from *Itgax*-DTA-*Prf1*$^{-/-}$ chimeric mice and WT-*Prf1*$^{-/-}$ controls 2 months after transplant. These percentages indicate the frequencies of each subpopulation out of the entire lymphogate in the organ (spleen or BM).

See also Table S1 and Figure S1.

RESULTS

Characterization of Perf-DCs in Radiation Chimeras

As previously described (Zangi et al., 2012), perf-DCs represent a minor subpopulation (~4%) within the CD11c^{+} population in the spleen of WT C57BL/6 mice (Figure S1A). This rare subpopulation of perf-DCs is markedly enhanced upon in vivo administration of GM-CSF (Zangi et al., 2012), and to a lesser extent, upon treatment with Flt3L (data not shown). Furthermore, as shown in Figure S1B, perforin is expressed in CD11c^{hi}MHC-II^{hi} DCs but not in CD11c^{int} macrophages identified by their F4/80 expression and by their inability to effectively stimulate T cells.

To evaluate the functional role of perf-DCs in the steady state in vivo, we generated mice that selectively lack perforin expression in CD11c^{hi} DCs. Chronic selective ablation of these cells can be attained in transgenic mice expressing the diphtheria toxin (DTx) A subunit (DTA) under control of a CD11c promoter (CD11c^{Cre}:R26-STOP-DTA mice [Birnberg et al., 2008]). Of note, most macrophages, NK cells, and pDCs, expressing low to intermediate CD11c, are spared in these mice (Birnberg et al., 2008). To induce a restricted perforin deficiency within the CD11c^{hi} DC population, we generated bone marrow (BM) chimeras using a 1:1 mixture of *Prf1*$^{-/-}$ BM (Kägi et al., 1994) and BM of mice expressing diphtheria toxin alpha chain (DTA) in CD11c^{hi} cells (*Itgax*-DTA mice) (Birnberg et al., 2008). Based on the reported properties of the *Itgax*-DTA mice (Birnberg et al., 2008), cells other than CD11c^{hi} DCs will be derived in the resulting chimeras (*Itgax*-DTA-*Prf1*$^{-/-}$), from both types of donor BM (and hence 50% will express perforin). In contrast, due to the DTA-mediated ablation of perforin-proficient cells, the CD11c^{hi} population will be exclusively derived from the *Prf1*$^{-/-}$ donor and therefore lack perforin. These chimeras should thereby allow us to determine whether the absence of perf-DCs leads to a particular autoimmune phenotype, similarly to that found in mice lacking other immune regulatory cells (Sakaguchi, 2000). In parallel, we generated control BM chimeras by transplantation of a 1:1 mixture of BM from *Prf1*$^{-/-}$ mice and BM from *Itgax*-DTA-negative littermates (WT-*Prf1*$^{-/-}$ mice). Histological evaluation via ImageJ software of cDCs isolated from spleens of *Itgax*-DTA-*Prf1*$^{-/-}$ chimeras confirmed absence of perforin-expressing DCs (0.09% ± 0.19%), whereas in WT-*Prf1*$^{-/-}$ chimera the expression of perf-DCs was reduced to 2.4% ± 1.9% from 4.1% ± 1% found in WT mice (data not shown).

Confirming our ablation strategy, CD11c^{hi}MHC-II^{hi} cDCs (Figure 1A), although reaching the same steady-state expression as in the WT-*Prf1*$^{-/-}$ chimera (Figure 1B), were exclusively derived from the CD45.2^{+} *Prf1*$^{-/-}$ donor (Figure 1C). Likewise,

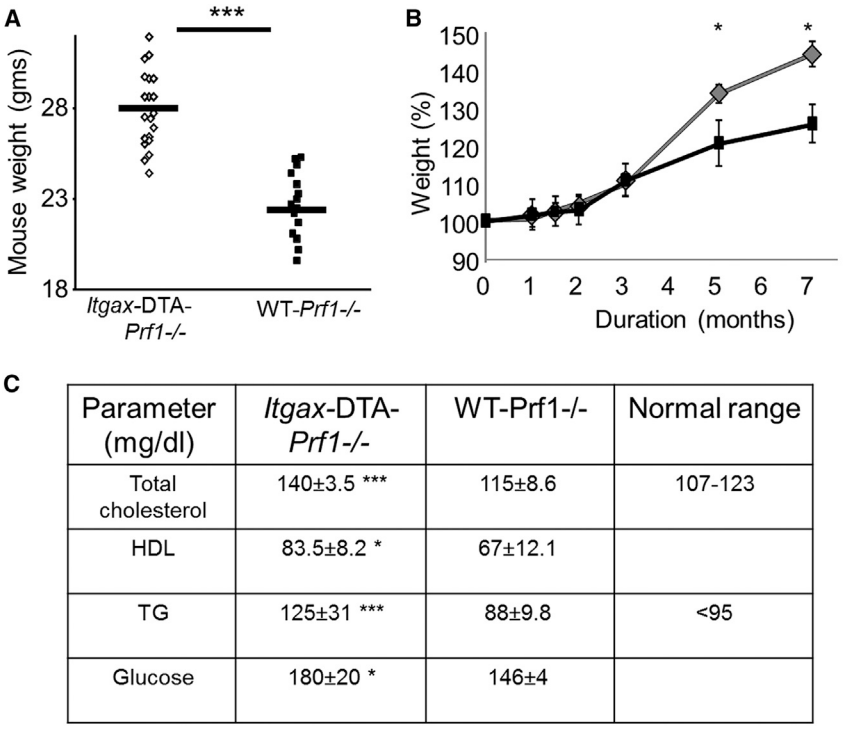

C

Parameter (mg/dl)	*Itgax*-DTA-*Prf1*-/-	WT-Prf1-/-	Normal range
Total cholesterol	140±3.5 ***	115±8.6	107-123
HDL	83.5±8.2 *	67±12.1	
TG	125±31 ***	88±9.8	<95
Glucose	180±20 *	146±4	

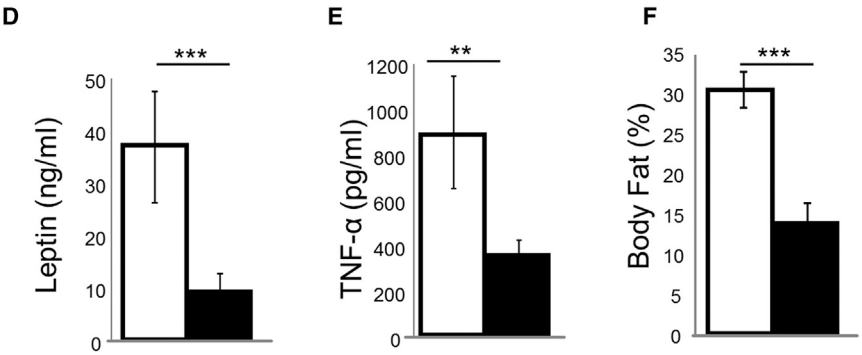

Figure 2. *Itgax*-DTA-*Prf1*$^{-/-}$ Mice Develop a Condition Resembling Metabolic Syndrome at 6 Months after Transplant

(A) Body weight of chimeric mice 6 months after transplant. Data pooled from three independent experiments (n ≥ 18).

(B) Kinetics of weight gain in *Itgax*-DTA-*Prf1*$^{-/-}$ (gray curve) and WT-*Prf1*$^{-/-}$ (black curve) mice. Error bars represent mean ± SD.

(C) Blood chemistry profile of the chimeric mice (mean ± SD, n ≥ 6, *p < 0.05, ***p < 0.001).

(D and E) Serum leptin (D) and TNF-α (E) amounts in the *Itgax*-DTA-*Prf1*$^{-/-}$ and control WT-*Prf1*$^{-/-}$ chimeras (mean ± SD, n ≥ 5).

(F) Percent body fat measured via EchoMRI. Error bars represent mean ± SD; *p < 0.05, ***p < 0.001 (open bar, *Itgax*-DTA-*Prf1*$^{-/-}$; closed bar, WT-*Prf1*$^{-/-}$).

Data are representative of three (A–D) or two (E and F) independent experiments. See also Figure S2.

BM pre-DCs largely originated from the CD45.2^{+} *Prf1*$^{-/-}$ donor (Figure 1D). In contrast, WT-*Prf1*$^{-/-}$ chimeras exhibited CD11c^{hi} cells that were equally derived from both BM donors (Figure 1D). Notably, T cells, B cells, neutrophils, pDCs, NK cells, and macrophages in the spleen of *Itgax*-DTA-*Prf1*$^{-/-}$ chimeras were equally derived from both BM donors (Figure 1E, Table S1). These results establish that *Itgax*-DTA-*Prf1*$^{-/-}$ chimeras, in which all CD11c^{hi} DCs are derived from *Prf1*$^{-/-}$ donors, and thus do not express perforin, offer a robust model for studying the role of perf-DCs in the steady state.

Perf-DC-Deficient Chimeras Develop Metabolic Syndrome

After the generation of *Itgax*-DTA-*Prf1*$^{-/-}$ chimeras, these mice were followed for a prolonged period to assess the development of a potential pathological phenotype that might be associated with the lack of perf-DCs. *Itgax*-DTA-*Prf1*$^{-/-}$ chimeric mice spontaneously gained significantly more weight compared to their WT-*Prf1*$^{-/-}$ counterparts, starting at ~5 months after transplant (Figures 2A and 2B). A similar difference was found when comparing the animals to an additional control group in which recipient mice received mixed BM from WT and *Itgax*-DTA donors (*Itgax*-DTA-WT) (Figure S2). The increased weight gain observed in *Itgax*-DTA-*Prf1*$^{-/-}$ mice prompted us to test whether this phenomenon was accompanied by metabolic alterations. Indeed, we detected dyslipidemia in the *Itgax*-DTA-*Prf1*$^{-/-}$ mice, manifested by elevated serum cholesterol and triglycerides in comparison to those exhibited by the controls (Figure 2C). In addition, the percent of total body fat, as measured by body composition MRI, was significantly elevated in *Itgax*-DTA-*Prf1*$^{-/-}$ mice compared to both control groups (Figure 2). *Itgax*-DTA-*Prf1*$^{-/-}$ mice, but not the control chimeras, displayed highly elevated TNF-α (linked to obesity-associated inflammation and insulin resistance) (Hotamisligil et al., 1993) and leptin, the proinflammatory adipokine associated with obesity, overeating, hypertension, cardiovascular diseases, and metabolic syndrome (Figures 2D–2F; Ouchi et al., 2011). Furthermore, *Itgax*-DTA-*Prf1*$^{-/-}$ chimeric mice exhibited decreased ability to handle glucose challenge (assessed by glucose-tolerance test [GTT]) (Figure 3A), as well as reduced insulin sensitivity (determined by insulin-tolerance test [ITT]) (Figure 3B). Taken together, these findings support a tendency of *Itgax*-DTA-*Prf1*$^{-/-}$ chimeric mice to develop type 2 diabetes and a general condition resembling metabolic syndrome.

In healthy individuals, AT expansion occurs by enlargement of the fat pad mass through enhanced recruitment of adipocyte precursor cells that differentiate into small adipocytes, along with the recruitment of other stromal cell types. Subsequently, vascularization, minimal induction of extracellular matrix

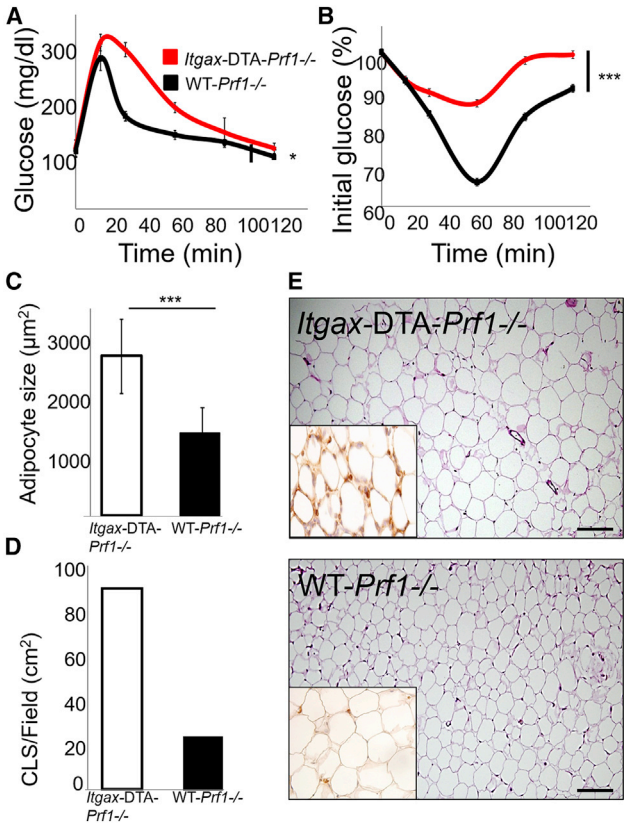

Figure 3. Typical Features of Type 2 Diabetes and Adipose Tissue Expansion in *Itgax*-DTA-*Prf1*$^{-/-}$ Mice

(A and B) Glucose homeostasis determined by glucose-tolerance test (A) and insulin-tolerance test (B) in *Itgax*-DTA-*Prf1*$^{-/-}$ (red) or WT-*Prf1*$^{-/-}$ (black) chimeric mice, demonstrating impaired glucose tolerance and reduced insulin sensitivity. Mice ($n \geq 6$ per group) were injected i.p. with 2 g glucose/kg body weight (BW) (A) or with 0.75 U insulin/kg BW (B), and plasma glucose was measured at the indicated time points. Mean ± SEM; statistical analysis was performed with GraphPad Prism software by repeated-measurements two-way ANOVA, followed by Bonferroni post hoc analysis; *$p < 0.05$, ***$p < 0.001$.

(C) Mean size of adipocytes in *Itgax*-DTA-*Prf1*$^{-/-}$ versus WT-*Prf1*$^{-/-}$ mice. The surface area of at least 100 adipocytes per image was counted, and a total of five images per epydidimal fat pad were analyzed by ImageJ software. Number of mice per group ≥ 3. Error bars represent mean ± SD.

(D) Number of CLSs per surface unit.

(E) Representative H&E staining of epydidimal fat pad from each group. Scale bars represent 50 µm.

Data are representative of three (A, B) or two (C, D) independent experiments.

(ECM), and minimal inflammation occur. In contrast, pathological expansion of AT is characterized by rapid growth of the fat pad through enlargement of existing fat cells, pronounced macrophage infiltration, limited vessel development, and massive fibrosis. Such pathological expansion is associated with chronic inflammation, ultimately resulting in the development of systemic insulin resistance (Sun et al., 2011). The observed metabolic syndrome in *Itgax*-DTA-*Prf1*$^{-/-}$ chimeras indicated that pathological AT expansion might occur in these mice. Indeed, as seen in Figures 3C–3E, adipocytes in the AT tissue of *Itgax*-DTA-*Prf1*$^{-/-}$ chimeras were larger, less organized, and more loosely packed compared to adipocytes in WT-*Prf1*$^{-/-}$ control chimeras. Moreover, the visceral AT of *Itgax*-DTA-*Prf1*$^{-/-}$ chimeras contained more "crown-like" structures (CLSs), which are formed when macrophages within inflamed AT cluster around dead adipocytes (Figures 3C–3E; Cildir et al., 2013).

CD4$^+$ and CD8$^+$ T Cells Are Required for Development of Metabolic Syndrome in *Itgax*-DTA-*Prf1*$^{-/-}$ Chimeras

To define candidate effector cells that might be controlled by perf-DCs, we initially analyzed immune cell populations in collagenase-digested stromal vascular fractions (SVF) from epididymal adipose tissue, as previously described (Brake et al., 2006).

WT-*Prf1*$^{-/-}$ and *Itgax*-DTA-*Prf1*$^{-/-}$ chimeras exhibited similar distributions of four subpopulations—CD11c^{hi}CD11b^{hi} (I), CD11c^{hi}CD11b^{int} (II), CD11c^{int}CD11b^{hi} (III), and CD11c^{int}CD11b^{int} (IV) cells in the AT—similar to the ones described above for the spleen. Although these subpopulations residing in the AT might differ in function and origin from the splenic cells bearing the same phenotypes, no significant difference in the frequencies of the CD11c^{hi} DCs was found between the two types of chimera (Figure S3). However, as shown in Figures 4A and 4B, AT of *Itgax*-DTA-*Prf1*$^{-/-}$ mice displayed significantly more CD4$^+$ and CD8$^+$ T cells compared to WT-*Prf1*$^{-/-}$ chimeras at 6 months after transplant, the time of disease onset, although no differences were found in neutrophil or macrophage numbers (Figure S3), nor in B or Treg cells (Figures 4C and 4D).

Because immune cell composition differed mainly in the T cell compartment, we further investigated the potential roles of CD4$^+$ and CD8$^+$ T cells by ablating these cell subpopulations prior to disease onset in the *Itgax*-DTA-*Prf1*$^{-/-}$ chimera. Because a developing inflammatory response was detected within the AT tissue based on cell composition (i.e., expansion of CD4$^+$ and CD8$^+$ T cells) and serum markers (leptin, TNF-α, IL-1β) starting at 5 months after transplant, we administered weekly i.p. injections of anti-CD4 antibodies, anti-CD8 antibodies, or both, starting 1 month prior to development of the earliest inflammatory signs (4th month after BM transplant). This treatment resulted in more than 95% depletion of the target population(s) in the spleen, LNs, and peripheral blood, with no changes in other cell populations (data not shown). More importantly, though, we found that *Itgax*-DTA-*Prf1*$^{-/-}$ mice treated with anti-CD4 antibodies, anti-CD8 antibodies, or a combination of them did not gain weight, similar to the WT-*Prf1*$^{-/-}$ controls (Figure 4E). Likewise, serum leptin was found to be elevated only in the group of *Itgax*-DTA-*Prf1*$^{-/-}$ mice not treated with antibody (Figure 4F). This observed role of both CD4$^+$ and CD8$^+$ T cells is consistent with potential triggering of the AT pathology by effector CD8$^+$ T cells requiring initial help from CD4$^+$ T cells.

Because alterations in central regulatory functions are probably involved in the metabolic changes observed, and recent data demonstrate changes in inflammatory status in the hypothalamus that might be important in body weight regulation, we evaluated the expression of interleukin-6 (IL-6) and IL-1β in the hypothalamus of *Itgax*-DTA-*Prf1*$^{-/-}$ and control WT-*Prf1*$^{-/-}$ chimeric mice before (4 months after transplant) and after (9 months after transplant) disease onset. We found that these cytokines were indeed elevated in *Itgax*-DTA-*Prf1*$^{-/-}$ chimera, albeit only after disease onset. Thus, although there was no significant difference at 4 months, by 9 months after transplantation

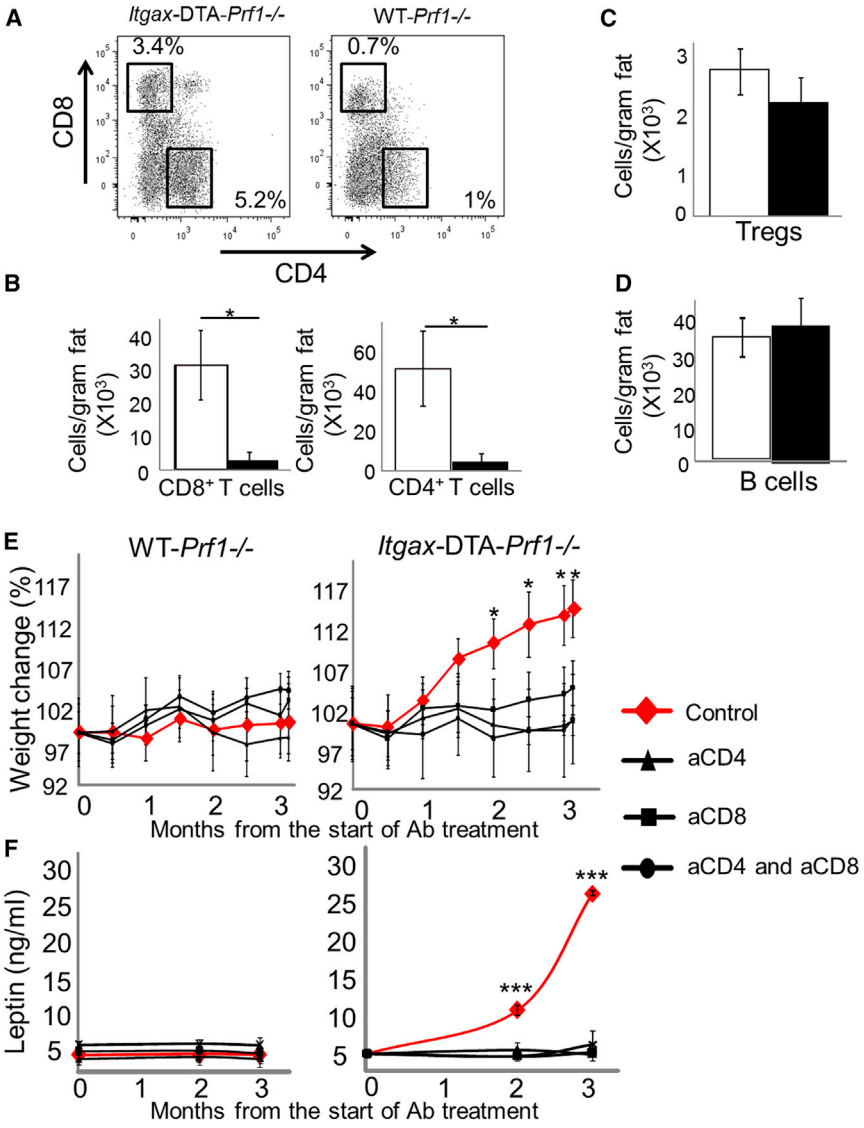

Figure 4. Elevated T Cell Numbers within AT of *Itgax*-DTA-*Prf1*$^{-/-}$ Mice 6 Months after Transplant; Systemic CD8$^+$ and CD4$^+$ Depletion Prevents Weight Gain and Increase in Leptin

SVF cells isolated from VAT of *Itgax*-DTA-*Prf1*$^{-/-}$ (white bars) and WT-*Prf1*$^{-/-}$ (black bars) mice maintained on a normal diet for 6 months were subjected to FACS analysis.

(A) Dot plots showing CD4$^+$ and CD8$^+$ T cells after gating out CD11b cells.

(B–D) Absolute numbers of CD4$^+$ and CD8$^+$ T cells (B), Treg cells (C), and B cells (D) were determined per gram of fat tissue (mean ± SD; *$p < 0.05$, $n \geq 5$).

(E) *Itgax*-DTA-*Prf1*$^{-/-}$ and WT-*Prf1*$^{-/-}$ mice were treated with weekly i.p. injections of anti-CD4 (black triangle), anti-CD8 (black square), or both antibodies (black circle). The control animals were treated with weekly injections of PBS (red diamond). The weight changes were monitored weekly and calculated as the percent of initial weight (mean ± SD; *$p < 0.05$).

(F) Leptin concentrations were measured by ELISA (mean ± SD; ***$p < 0.001$).

Data are representative of two replicates. See also Figure S3.

IL-6 was four times higher in *Itgax*-DTA-*Prf1*$^{-/-}$ mice compared to WT-*Prf1*$^{-/-}$ mice ($p < 0.01$), and IL-1β was six times higher in *Itgax*-DTA-*Prf1*$^{-/-}$ mice compared to WT-*Prf1*$^{-/-}$ mice ($p < 0.05$), indicating that these changes might be induced as a result of the inflammatory process in AT.

The T Cell Repertoire Is Modified within the Adipose Tissue of *Itgax*-DTA-*Prf1*$^{-/-}$ Chimeras

It is possible that autoimmune T cells are poorly controlled in the absence of regulatory perf-DCs. To address this possibility, the TCR repertoire from AT tissue of *Itgax*-DTA-*Prf1*$^{-/-}$ and WT-*Prf1*$^{-/-}$ chimeras at 6 months after transplant was analyzed by high-throughput TCR sequencing (Ndifon et al., 2012). We sequenced the TCRβ CDR3 region of T cells and compared the repertoire found in spleen, visceral AT (VAT), and subcutaneous AT (SC-AT) of *Itgax*-DTA-*Prf1*$^{-/-}$ and WT-*Prf1*$^{-/-}$ chimeras.

As a measure of the composition of the TCR repertoire, we evaluated the degree of skewing in the frequencies of observed TCR sequences. A more diverse repertoire consists of sequences that are found at similar frequencies, whereas in a skewed repertoire, a small number of sequences are dominant and are found at higher frequencies. The skewing of a repertoire can be evaluated by the increased deviation of its Lorentz curve from the diagonal. We first compared the repertoires of T cells resident within AT to the repertoire found in the spleen of WT-*Prf1*$^{-/-}$ animals. Consistent with previous observations of a restricted TCR repertoire within AT (Feuerer et al., 2009; Winer et al., 2009; Yang et al., 2010), we observed greater skewing in the repertoires of T cells derived from VAT and SC-AT compared with splenic T cells of WT-*Prf1*$^{-/-}$ mice (Figure 5A). We also identified specific Vβ segments that were enriched in the repertoires derived from AT compared with the splenic repertoire. Next, we compared the TCR repertoires between WT-*Prf1*$^{-/-}$ and *Itgax*-DTA-*Prf1*$^{-/-}$ chimeras. Although there was no difference in the spleens of these chimeras, the TCR repertoire observed in the AT tissues derived from *Itgax*-DTA-*Prf1*$^{-/-}$ mice was less skewed than that of the WT-*Prf1*$^{-/-}$ mice (Figure 5A). Thus, the TCR repertoire in AT of the WT-*Prf1*$^{-/-}$ chimera is dominated by expansion of a small number of clonotypes, whereas the *Itgax*-DTA-*Prf1*$^{-/-}$ AT repertoire contains a greater number of distinct T cell clones with intermediate expression. To identify signature TCR sequences that distinguish the two types of chimera, we used an ordination method, similar to principal-component analysis (Yeung and Ruzzo, 2001), termed redundancy analysis (RDA) (Sadyś et al., 2015). This method attempts to explain the variance in the data, constrained by the grouping of samples, by fitting a linear model that maximizes the variance between groups. With RDA,

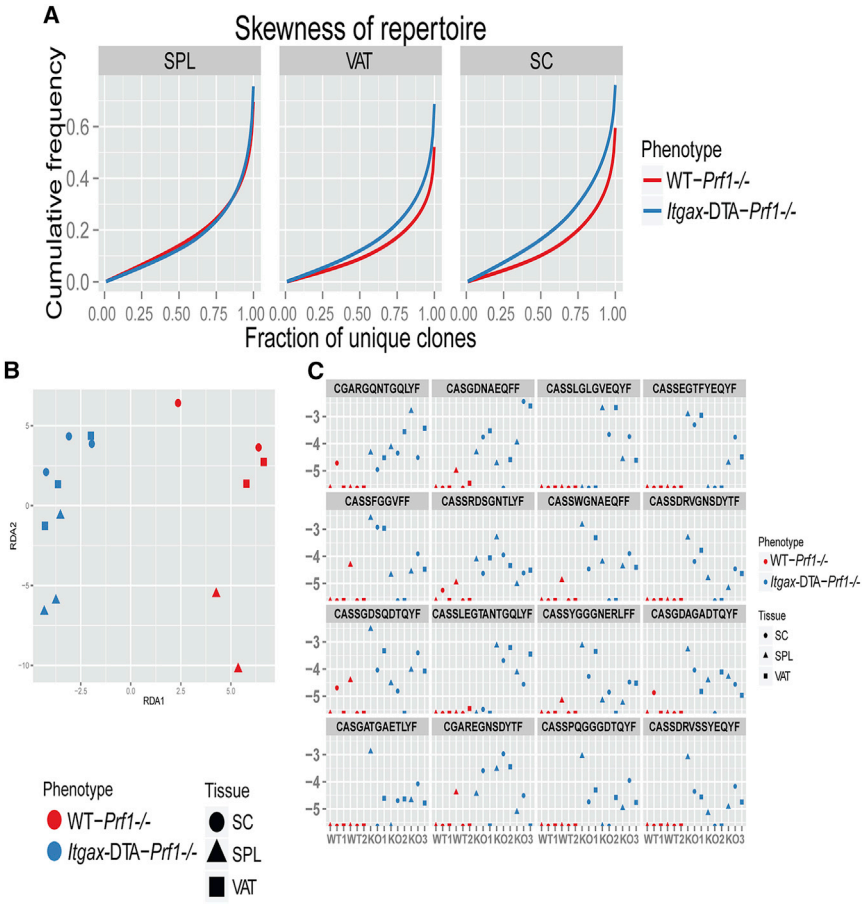

Figure 5. A Modified TCR Repertoire in Adipose Tissues from *Itgax*-DTA-*Prf1*$^{-/-}$ Mice Compared with WT-*Prf1*$^{-/-}$ Mice

(A) Lorenz representation of the TCRβ repertoire skewing for T cells from spleen, VAT, and SC-AT of *Itgax*-DTA-*Prf1*$^{-/-}$ (blue) and WT-*Prf1*$^{-/-}$ (red) mice. For each mouse, clonotypes were ordered by frequency. The cumulative frequency was then calculated at each rank (normalized to sample size). The curves represent the mean for each experimental group.

(B) Redundancy analysis (RDA) is an extension of principal-component analysis (PCA) that explicitly models response variables (most abundant CDR3 AA sequences, here) as a function of explanatory variables: sample type, mouse (*Itgax*-DTA-*Prf1*$^{-/-}$ or WT-*Prf1*$^{-/-}$), and tissue (spleen, VAT, SC-AT), in this case. This analysis separates between repertoires of *Itgax*-DTA-*Prf1*$^{-/-}$ (blue) versus WT-*Prf1*$^{-/-}$ (red) along RDA1, and between most spleen samples (triangles) versus adipose tissue samples (circles, SC; squares, VAT) along RDA2.

(C) RDA analysis identifying the CDR3 sequences that are most highly enriched in repertoires of perforin KO mice compared with WT. 16 CDR3β sequences with the lowest (negative) weights on RDA1. These clones were enriched in *Itgax*-DTA-*Prf1*$^{-/-}$ mice (blue, n = 3; all three tissues are shown for each mouse) compared with WT mice (red, n = 2).

See also Figure S4.

we selected TCR sequences with the highest contribution to the separation between the experimental groups, resulting in a list of signature sequences that were highly expressed in one group but not in the other. This analysis separated repertoires of *Itgax*-DTA-*Prf1*$^{-/-}$ versus WT-*Prf1*$^{-/-}$ mice along the first RDA axis (RDA1), and between most spleen samples versus VAT samples along RDA2 (Figure 5B). Next, we identified CDR3 sequences that were most highly enriched in repertoires of *Itgax*-DTA-*Prf1*$^{-/-}$ mice compared with WT-*Prf1*$^{-/-}$, by RDA analysis. Figure 5C shows 16 CDR3β amino acid sequences with the lowest (negative) weights on RDA1, which were enriched in *Itgax*-DTA-*Prf1*$^{-/-}$ mice compared with WT-*Prf1*$^{-/-}$ mice. Several TCRβ sequences were consistently upregulated across *Itgax*-DTA-*Prf1*$^{-/-}$ animals, suggesting their potential role in the observed phenotype. Of note, many of these TCRs are encoded by different nucleotide sequences in different animals (Figure S4), an indication of clonal selection driven by TCR specificity. These TCR sequences, which exist in the *Itgax*-DTA-*Prf1*$^{-/-}$ but not in the WT-*Prf1*$^{-/-}$ animals, might be mechanistically related to the metabolic phenotype, though further studies are required to identify the specificity of the TCRs that distinguish the two types of chimeras.

Itgax-DTA-*Prf1*$^{-/-}$ Chimeras Develop Enhanced Obesity in Response to a High-Fat Diet

To learn how mice lacking perf-DCs respond to excess adiposity, we used a classical model of obesity, in which mice are chronically fed a high-fat diet (HFD). When fed HFD, normal WT C57BL/6 mice develop glucose intolerance and insulin resistance by the 12th week, with elevated pro-inflammatory cytokines and adipokines. *Itgax*-DTA-*Prf1*$^{-/-}$ mice have a tendency to spontaneously develop these symptoms, so we followed the dynamics of metabolic and functional changes at early time points. As can be seen in Figures 6A and 6B, *Itgax*-DTA-*Prf1*$^{-/-}$ mice gained weight much earlier than WT-*Prf1*$^{-/-}$ chimeras when fed HFD, with higher percentage of body fat, increased liver weight, and epididymal fat pad weight (Figures 6C–6E).

Furthermore, serum leptin was significantly higher as early as 1 month after initiation of HFD. At 1.5 months from initiation of feeding, insulin and both IL-1β and tumor necrosis factor-α (TNF-α) were elevated in *Itgax*-DTA-*Prf1*$^{-/-}$ mice (Figures 6F–6H and 6L). Plasma cholesterol and triglycerides were elevated in *Itgax*-DTA-*Prf1*$^{-/-}$ mice relative to control WT-*Prf1*$^{-/-}$ animals, starting at 1 month from initiation of HFD (Figure 6F), and liver TGs were also markedly higher (Figures 6I–6K). Thus, the increased susceptibility to diet-induced obesity could offer an additional, more rapid model for investigating the impact of perf-DCs on different immune cell subpopulations.

As in the normal-fat diet, we also found that larger numbers of both CD8$^+$ and CD4$^+$ T cells infiltrated the VAT in *Itgax*-DTA-*Prf1*$^{-/-}$ mice fed with HFD compared to controls (Figure S5). Although there was no significant elevation of macrophages within the VAT of the *Itgax*-DTA-*Prf1*$^{-/-}$ chimera (Figure S5), we found by RT-PCR a significant shift toward a gene expression profile typical of inflammatory M1 macrophages (Figure 6J), which is consistent

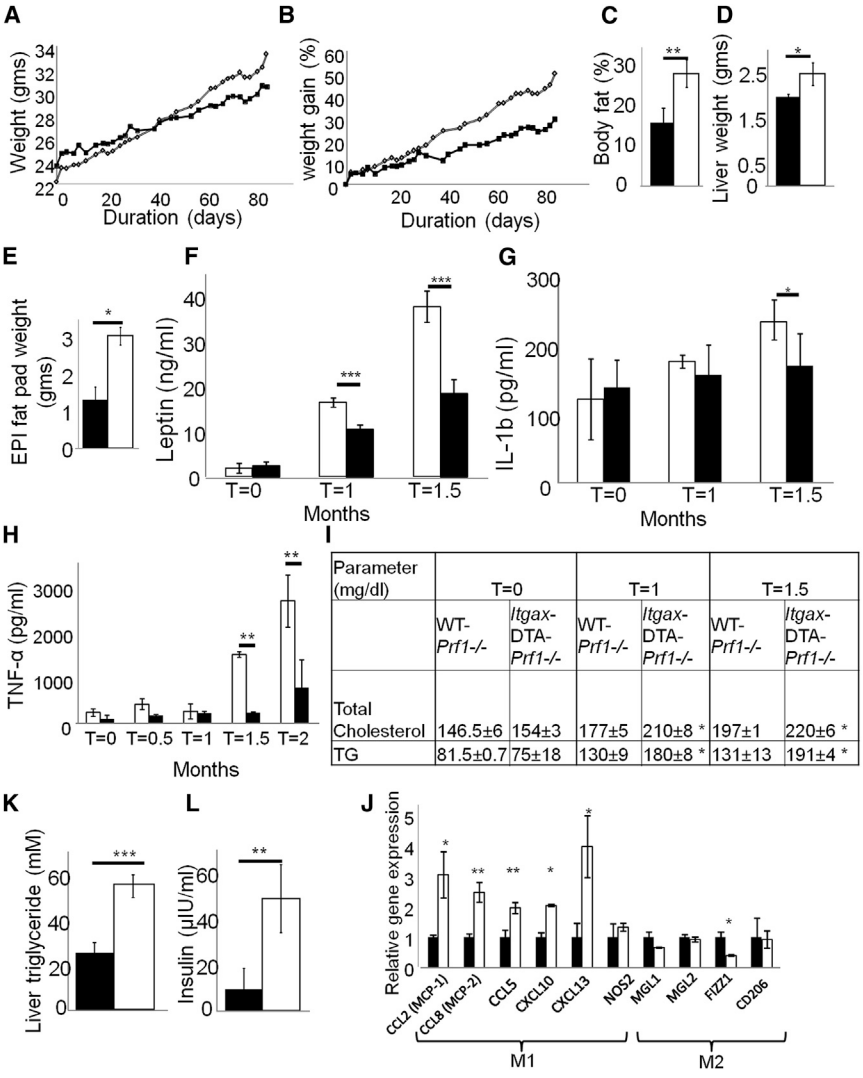

Figure 6. *Itgax*-DTA-*Prf1*$^{-/-}$ Chimeras Are More Prone to HFD-Induced Inflammation

(A and B) 2 months after chimerism induction, *Itgax*-DTA-*Prf1*$^{-/-}$ (gray) and WT-*Prf1*$^{-/-}$ (black) chimeras were maintained on HFD and monitored for weight change (numbers in A and percent in B) over 90 days.

(C–E) Percent of body fat (C), liver weight (D), and epididymal fat pad weight (E) in *Itgax*-DTA-*Prf1*$^{-/-}$ (white) and WT-*Prf1*$^{-/-}$ (black) chimeras maintained for 6 weeks on HFD (mean ± SD; *$p < 0.05$; **$p < 0.01$).

(F–H) Amounts of leptin (F), IL-1β (G), and TNF-α (H) were tested in sera of *Itgax*-DTA-*Prf1*$^{-/-}$ (white) and WT-*Prf1*$^{-/-}$ (black) chimeras maintained on high and low fat. Blood was drawn at different time points, as indicated (mean ± SD; *$p < 0.05$, ***$p < 0.001$, $n \geq 5$).

(I) Serum cholesterol and TG in chimeric mice fed HFD (mean ± SD, $n \geq 5$).

(J) Gene expression profile of M1 versus M2 genes determined by RT-PCR in VAT of *Itgax*-DTA-*Prf1*$^{-/-}$ (white) and WT-*Prf1*$^{-/-}$ (black) chimeras, maintained on HFD for 2 months (mean ± SD; *$p < 0.05$; **$p < 0.01$).

(K) Liver triglycerides in *Itgax*-DTA-*Prf1*$^{-/-}$ (white) and WT-*Prf1*$^{-/-}$ chimera maintained for 6 weeks on HFD (mean ± SD, $n \geq 4$).

(L) Serum insulin in *Itgax*-DTA-*Prf1*$^{-/-}$ (white) and WT-*Prf1*$^{-/-}$ chimeras maintained for 6 weeks on HFD (mean ± SD, $n \geq 4$).

Data are representative of three (A–F) or two (G–L) independent experiments. See also Figures S5–S7.

with increased inflammatory properties of macrophages in the AT of obese mice (Lumeng et al., 2007a; Weisberg et al., 2003).

It is possible that activation of T and NK cells upon onset of inflammation or initiation of HFD might induce upregulation of CD11c, and thereby of DT to a degree sufficient to cause the deletion of these populations. Clearly, such deletion would not be apparent in analysis of cell populations in the naive mice, shown in Figure 1 prior to onset of disease. We therefore re-evaluated potential changes in the level of *Prf1*$^{-/-}$-derived cells within various leukocyte populations in the BM, spleen, and VAT before (2 months after BMT) and after (7 months after BMT) the onset of the metabolic phenotype. Likewise, we analyzed such potential changes in chimeric mice after 8 weeks of HFD, by which time the full-blown syndrome develops in *Itgax*-DTA-*Prf1*$^{-/-}$ mice. As shown in Figures S6 and S7 and Table S1, the relative abundance of the various cell types found in naive mice remained unaltered after the inflammatory onset. These findings are in line with previous observation, showing that T cells from *Itgax*-DTA-*Prf1*$^{-/-}$ mice respond normally to antigen challenge and are not deleted upon activation (Birnberg et al., 2008).

Perf-DCs Exhibit a Major Regulatory Role in EAE

We showed that selective deletion of perforin in the rare subpopulation of perf-DCs leads to a distinct metabolic phenotype and that this phenotype can be prevented by T cell depletion in vivo. This strongly indicates a role for perf-DCs in the control of T-cell-mediated inflammatory processes. However, although we found a skewed TCR repertoire exhibited by AT T cells in *Itgax*-DTA-*Prf1*$^{-/-}$ chimeras, the identity of antigens eliciting this inflammatory response are not known. To further investigate the regulatory role of perf-DCs, we evaluated whether perf-DCs might also exhibit a regulatory role in a well-defined mouse model for autoimmunity, in which the pathological antigen is known. We therefore examined whether *Itgax*-DTA-*Prf1*$^{-/-}$ chimeras are more susceptible to development of EAE, a T-cell-mediated disorder widely used as a model of multiple sclerosis (Aharoni, 2013). In this mouse model, MOG-induced EAE results in a chronic persistent disease course.

MOG administration in *Itgax*-DTA-*Prf1*$^{-/-}$ mice resulted in a greater clinical severity of the disease with earlier onset and higher disease score (Figures 7A and 7B). Moreover, lymph node cells from *Itgax*-DTA-*Prf1*$^{-/-}$ mice showed more antigen-specific proliferation of CD4$^+$ T cells, both during the peak of the disease at day 14 and during the chronic stage at day 30. This specificity is clearly illustrated when comparing the marked

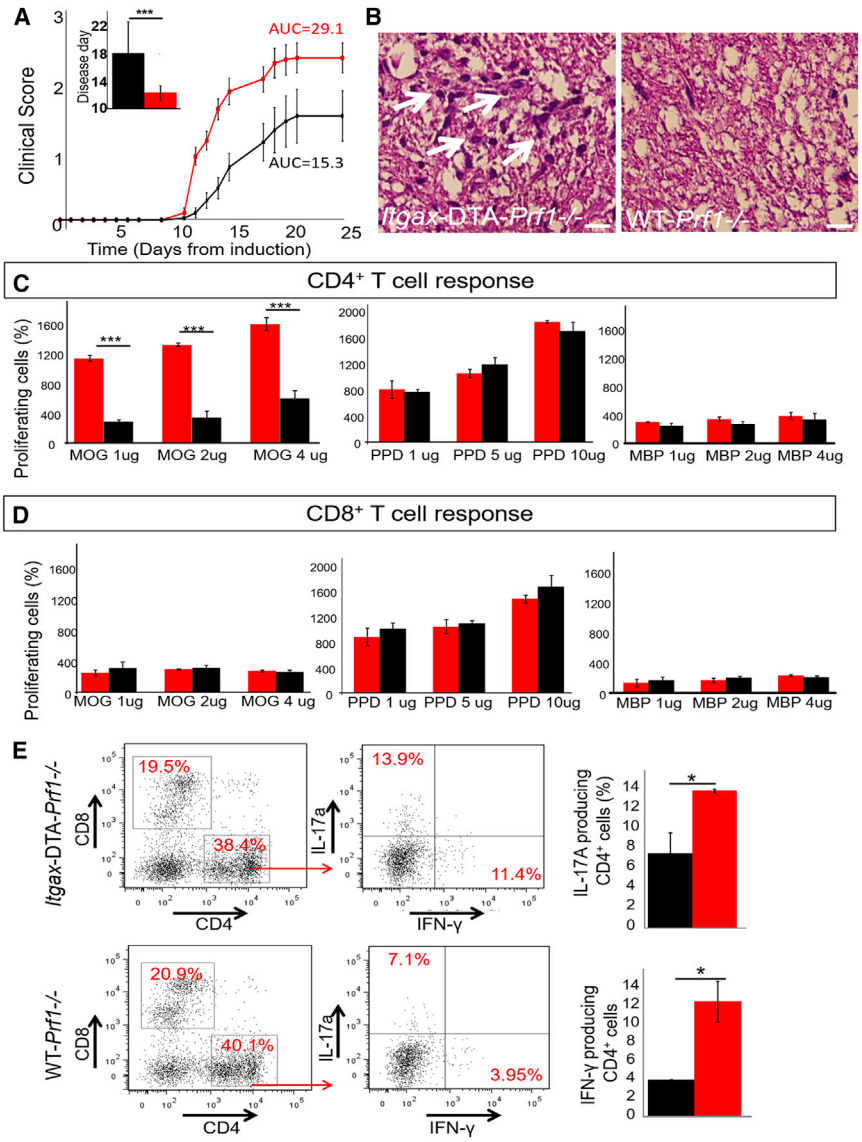

Figure 7. Perforin Deficiency within the DC Population Results in Enhanced Susceptibility to EAE

(A) Disease progression of *Itgax*-DTA-*Prf1*$^{-/-}$ (red) and WT-*Prf1*$^{-/-}$ (black) mice immunized with MOG, and the average day of EAE onset (mean ± SEM of two experiments with a total of 18 mice per group).

(B) Spinal cord sections from the mice described in (A), stained with hematoxylin and eosin (H&E); arrows indicate inflammatory infiltrates. Scale bars represent 10 μm.

(C and D) MOG-specific proliferation of splenocytes from *Itgax*-DTA-*Prf1*$^{-/-}$ (red) and WT-*Prf1*$^{-/-}$ (black) mice 30 days after immunization. Proliferation was assessed by CFSE dilution together with CD4 and CD8 antibody staining by flow cytometry (***$p < 0.001$; mean ± SD, 5 mice per group).

(E) Analysis of spinal cord T cells. T cells were isolated from 3–5 pooled spinal cords from the *Itgax*-DTA-*Prf1*$^{-/-}$ or WT-*Prf1*$^{-/-}$ mice, 14 days after immunization with MOG, stimulated with soluble CD3 overnight, and then stained for IL-17a and IFN-γ (mean ± SD; *$p < 0.05$, $n \geq 3$).

Data are representative of two independent experiments.

enhancement of anti-MOG CD4$^+$ T cells to that exhibited by T cells directed against PPD or MBP (Figure 7C) or of CD8$^+$ T cells directed against MOG (Figure 7D). MOG-specific IFN-γ- and IL-17A-positive T cells were also found in the central nervous system (CNS) 14 days after immunization (Figure 7E). These results demonstrate the immune-regulatory role of perf-DCs and the ability of these cells to inhibit detrimental expansion of antigen-specific autoimmune clones in the context of EAE.

DISCUSSION

We have shown here that DCs expressing perforin represent a subpopulation of regulatory DCs with a steady-state role in prevention of inflammatory processes within the AT and in the CNS. The intriguing relationship between metabolism and the immune system has received increasing attention over the past few years (Schipper et al., 2012). AT is now recognized as a true endocrine organ that plays a fundamental role in controlling whole-body glucose and lipid homeostasis (Guilherme et al., 2008). Previous studies have identified various immune cells as metabolic controllers with pathogenic or regulatory potential (Chawla et al., 2011; Elgazar-Carmon et al., 2008; Feuerer et al., 2009; Kang et al., 2008; Liu et al., 2009; Lumeng et al., 2007a, 2007b; Nguyen et al., 2007; Nishimura et al., 2013; Odegaard et al., 2007; Osborn and Olefsky, 2012; Talukdar et al., 2012; Wu et al., 2011). Three T lymphocyte subsets might play distinct roles in AT immune homeostasis: CD8$^+$ T cells (Nishimura et al., 2009), IFN-γ$^+$CD4$^+$ T (Th1) cells (Rocha et al., 2008; Winer et al., 2009), and Foxp3$^+$ regulatory T (Treg) cells (Eller et al., 2011; Feuerer et al., 2009; Ilan et al., 2010). In particular, the infiltration of CD8$^+$ T cells to the AT has been shown to precede macrophage influx and M1 polarization in the obese AT (Nishimura et al., 2009; Rausch et al., 2008), and CD8$^+$ T cells are involved in macrophage recruitment and polarization in obesity (Nishimura et al., 2009). Furthermore, as also shown here, depletion of CD8$^+$ T cells in obese mice improved insulin sensitivity, whereas adoptive transfer of CD8$^+$ T cells induces insulin resistance in CD8-deficient mice (Nishimura et al., 2009).

A major drawback of most of these studies is the reliance on HFD, which does not accurately represent normal steady-state conditions in the AT. Our study showed the major impact of a unique DC subpopulation on AT inflammatory processes in the context of normal dietary conditions. The HFD regimen is associated with further acceleration of disease onset in *Itgax*-DTA-*Prf1*$^{-/-}$ chimeras that lack perf-DCs and are susceptible to AT

inflammation. Our observations of differences in TCRβ repertoires of WT-*Prf1*$^{-/-}$ versus *Itgax*-DTA-*Prf1*$^{-/-}$ mice in both adipose tissues tested (VAT and SC-AT), but not in the spleen, suggest that specific T cells are missing from the adipose tissue of WT-*Prf1*$^{-/-}$ animals, potentially due to their deletion by regulatory perf-DCs. The possibility that the phenotype might be mediated by antigen-specific T cells that escape regulation in the absence of perf-DCs is supported by the observation that the inflammatory AT phenotype can be completely prevented by T cell depletion using either anti-CD4 or anti-CD8 antibodies. As expected from previous studies in mice fed HFD (De Souza et al., 2005), this inflammatory process is also accompanied by late increase in IL-6 and IL-1B expression in the hypothalamus. However, the late onset of this process in *Itgax*-DTA-*Prf1*$^{-/-}$ chimeras indicates that it might be induced by the phenotype rather than cause it.

In our chimeric mouse model, the T cell compartment must reconstitute itself after transfer of BM to irradiated recipients. Such reconstitution is slow, requiring about 2 months in mice. Thus, we expect a delay in the replenishment of fat-resident T cells at least of that magnitude, and possibly even longer, due to slower traffic of T cells into the fat tissue. Only when sufficient numbers of self-reactive T cells accumulate in the fat tissue are inflammatory processes initiated.

Considering that DTA mice tend to develop a myeloproliferative disorder at old age, it could be argued that such a pathological process might be somehow associated with the phenotype observed in our *Itgax*-DTA-*Prf1*$^{-/-}$ chimera, which also develops late after transplantation. However, we did not detect in our chimeric mice any sign of myeloproliferative disorder, in line with Birnberg et al. (2008), who showed in their original paper that this phenotype did not develop in BM chimera established by combining BM from DTA mice with BM from WT mice.

The *Itgax* promoter is also active in cells other than DCs, including some NK cells, macrophages, and pDCs, although the specific *Itgax* promoter fragment used for the *Itgax*-cre transgenic mice is inactive in certain cells (CD11c^{int} moDCs, CD11c^{int} PDCs, and NK cells) that transcribe their endogenous *Itgax* alleles (Bar-On and Jung, 2010). Nevertheless, we extensively evaluated the possibility that our observed phenotype might be associated with ablation of these cells in our *Itgax*-DTA-*Prf1*$^{-/-}$ chimera. Thus we studied in our *Itgax*-DTA-*Prf1*$^{-/-}$ and WT-*Prf1*$^{-/-}$ chimeras the expression of markers associated with NK cells (NK1.1, NKp46, and CD49b(DX5)), macrophages (F4/80), and pDCs (PDCA-1), and we confirmed the previous suggestion of Bar-On and Jung (2010) that these cells, which express intermediate or low CD11c, are not ablated by DTA. Thus, they are equally derived in the *Itgax*-DTA-*Prf1*$^{-/-}$ chimera from both BM donors.

These results are in line with our previous work on perf-DCs generated in vitro from hematoipoietic stem cells (HSCs), negating the possibility of overlap between these cells and the so-called natural killer dendritic cells (NKDCs) or interferon-producing killer dendritic cells (IKDCs), previously reported to exhibit dual NK and DC properties (Chan et al., 2006; Pillarisetty et al., 2005; Taieb et al., 2006) or activated NK cells (Blasius et al., 2007; Vosshenrich et al., 2007), as we demonstrated that perf-DCs do not express markers typically associated with NK cells, such as NK1.1, DX5, and NKp46, and are negative for B220, which is expressed by IKDCs.

It could be argued that if indeed ablation of perf-DCs is critical for our observed phenotype, one would expect that *Prf1*$^{-/-}$ mice, in which the mutation is expressed in every cell, would be similarly susceptible to obesity. However, in such mice both parts of the equation are impacted. Thus, not only perf-DCs, but also perforin-positive effector T cells or NK cells critical for inflammation, are missing, and therefore it is hard to predict the overall outcome. In fact, in parallel to the submission of our manuscript, a new study was published suggesting that *Prf1*$^{-/-}$ mice exhibit enhanced obesity and some metabolic disturbances (Revelo et al., 2015). However, we observed only minor weight gain with no increase in cholesterol or TG, and no changes in the ability to handle glucose and insulin challenges compared to WT mice (not shown).

Taken together, our results suggest that under physiological conditions, perf-DCs probably induce deletion of specific self-reactive T cells, potentially through presentation of tissue-specific self-antigens. In the case of adipose tissue, this leads to deletion of tissue-resident T cells that have inflammatory capacity, thereby contributing to immune tolerance. Thus, the appearance of metabolic syndrome upon specific ablation of perf-DCs in our experiments appears to be a consequence of reduced deletion of those harmful T cells, resulting in adipose inflammation. Furthermore, our results strongly suggest that in the steady state, a unique population of perf-DCs attenuates the severity of EAE by specifically controlling CD4^{+} T cells that produce IL-17 and IFN-γ upon activation by their cognate antigen.

The results shown in the present study collectively demonstrate that perf-DCs exhibit an essential role in regulating the delicate balance between immune cells and the fat tissue, and consequently, the entire cascade leading to metabolic syndrome and its associated type 2 diabetes. Thus, we suggest that future therapies could operate by shifting the homeostatic balance of perf-DC abundance and that of other immune cell populations, and their activation state. This might be attained either by inhibiting their ecological competitors or by giving them a growth or accumulation advantage. Our insights regarding the role of perf-DCs might offer opportunities for new rational therapeutics, directed not only at controlling aberrant T cell clones, but also at addressing the regulatory possibilities offered by perf-DCs.

Perforin deficiency within the myeloid DC population results in enhanced susceptibility to EAE. Therefore, perf-DCs might represent, in addition to Treg cells, a regulatory cell population, critical for protection from autoimmunity and AT inflammatory processes. Further studies of these regulatory cells in normal human subjects and in patients is required to establish the translational value of our findings, which could potentially lead to important therapeutic approaches.

EXPERIMENTAL PROCEDURES

Animals

Mice were 6- to 12-week-old females or males of the following strains: C57BL/6, *Itgax*-DTA, and *Prf1*$^{-/-}$ (Weizmann Institute Animal Breeding Center). BM chimeras were generated by exposure of C57BL/6 WT mice to a single dose of 950 rad total body irradiation. The following day, the mice received 5 × 10^{6} mixed BM cells i.v., as indicated. Animals were maintained under conditions approved by the Institutional Animal Care and Use Committee at the Weizmann Institute of Science. In some experiments, mice were maintained on high-fat diet as detailed in the Supplemental Experimental Procedures.

Metabolic Studies

Itgax-DTA-*Prf1*$^{-/-}$ and WT-*Prf1*$^{-/-}$ chimeric mice were weighed regularly. Tests for glucose and insulin tolerance, glucose, triglycerides, total cholesterol, high-density lipoprotein (HDL), and cytokine serum levels (measured by ELISA kits) are detailed in the Supplemental Experimental Procedures. Body composition analysis was performed by EchoMRI Analyzer (EchoMRI).

Fat-Associated SVF Cell Isolation

VAT and inguinal SC pads were mashed into small pieces, and single-cell suspensions were prepared by collagenase digestion, as detailed in the Supplemental Experimental Procedures.

Histology, Immunohistochemistry, and Cytofluorometric Analysis

Tissue samples from spinal cord and visceral adipose tissue were fixed, processed, and embedded in paraffin. Sections of 5 μm were stained with hematoxylin and eosin (H&E). Fat cell area on H&E-stained slides was measured with ImageJ software as detailed in the Supplemental Experimental Procedures. Staining of perforin to identify perf-DCs is described in the Supplemental Experimental Procedures. In brief, splenic DCs from WT and *Prf1*$^{-/-}$ mice were isolated by two-stage magnetic sorting and were spun onto glass slides and fixed with 4% PFA. The cells were then blocked first with 5% horse serum and 0.2% Triton for 5 min, and subsequently with 100% horse serum for 1 hr. Isotype blocking was done with rat IgG2a overnight in 25% horse serum and 0.1% Triton at 4°C followed by secondary anti-RatCy2 or anti-Rat DyLight594 (Jackson) antibody to visualize the non-specific binding. Specific rat anti-perforin Ab (Clone CB5.4, Abcam) was applied overnight in 25% horse serum and 0.1% Triton at 4°C followed by secondary anti-rat DyLight 594 or anti-rat AMCA (Jackson) antibody. The nuclei were stained with Hoechst blue or yellow stain. Flow cytometry and analysis are outlined in the Supplemental Experimental Procedures.

Depletion of CD4$^+$ and CD8$^+$ T Cell Populations

Anti-CD4 or -CD8 depleting antibodies were administered i.p. weekly, as detailed in the Supplemental Experimental Procedures.

RNA Extraction, Quantitative RT-PCR for AT, and TCRβ Sequencing

Total RNA from fat pads was extracted and reverse-transcribed as detailed in the Supplemental Experimental Procedures. Total RNA was extracted from spleen, visceral adipose tissue, and subcutaneous adipose tissue of DTA-PKO and WT-PKO mice. The TCRβ sequencing procedure and computational analysis are detailed in the Supplemental Experimental Procedures.

EAE Induction and Evaluation

Chronic EAE was induced in C57BL/6 chimeric mice by injecting a peptide consisting of amino acids 35–55 of myelin oligodendrocyte glycoprotein (MOG) as detailed in the Supplemental Experimental Procedures. Mice were examined daily and EAE was scored as follows: 0, no disease; 1, limp tail; 2, hind limb paralysis; 3, paralysis of all limbs; 4, moribund condition; and 5, death.

CFSE Proliferation Assay of CD4$^+$ and CD8$^+$ T Cells

Isolated lymph node cells from chimeric mice 14 or 30 days after EAE induction were isolated and stained with 5 μM CFSE (CellTrace CFSE Cell Proliferation Kit, Invitrogen) for 15 min. Proliferation in response to different stimuli was assessed, as detailed in the Supplemental Experimental Procedures.

SUPPLEMENTAL INFORMATION

Supplemental Information includes seven figures, two tables, and Supplemental Experimental Procedures and can be found with this article online at http://dx.doi.org/10.1016/j.immuni.2015.08.015.

AUTHOR CONTRIBUTIONS

Writing - Original Draft, Y.Z.K., B.N.L., and Y.R.; Review & Editing, S.J., N.F., R. Arnon, and Y.R.; Methodology, Y.Z.K., B.N.L., and Y.R.; Conceptualization, Y.Z.K. and Y.R.; Investigation, Y.Z.K., B.N.L., E. Shezen, C.R., S.K., E. Shifrut, S.R.-Z., R. Aharoni, O.Y., and A.A.; Resources, S.J. and L.B.; Formal Analysis, E. Shifrut and N.F.; Supervision, Y.R.; Funding Acquisition, Y.R.

ACKNOWLEDGMENTS

The authors wish to thank Dr. Eran Elinav for reviewing the manuscript and Dr. Hagit Shapiro, Dr. Yael Kuperman, and Dr. Michael Tsoory for professional advice. Y.R. holds the Henry Drake Professorial Chair in Transplantation Immunology. This work was supported in part by grants from BIRAX (Britain-Israel Research and Academic Exchange) Regenerative Medicine Initiative and ISF (no. 1346/14) and from Roberto and Renata Ruhman.

Received: October 20, 2014
Revised: May 27, 2015
Accepted: August 14, 2015
Published: September 15, 2015

REFERENCES

Aharoni, R. (2013). New findings and old controversies in the research of multiple sclerosis and its model experimental autoimmune encephalomyelitis. Expert Rev. Clin. Immunol. *9*, 423–440.

Bar-On, L., and Jung, S. (2010). Defining dendritic cells by conditional and constitutive cell ablation. Immunol. Rev. *234*, 76–89.

Birnberg, T., Bar-On, L., Sapoznikov, A., Caton, M.L., Cervantes-Barragán, L., Makia, D., Krauthgamer, R., Brenner, O., Ludewig, B., Brockschnieder, D., et al. (2008). Lack of conventional dendritic cells is compatible with normal development and T cell homeostasis, but causes myeloid proliferative syndrome. Immunity *29*, 986–997.

Blasius, A.L., Barchet, W., Cella, M., and Colonna, M. (2007). Development and function of murine B220+CD11c+NK1.1+ cells identify them as a subset of NK cells. J. Exp. Med. *204*, 2561–2568.

Brake, D.K., Smith, E.O., Mersmann, H., Smith, C.W., and Robker, R.L. (2006). ICAM-1 expression in adipose tissue: effects of diet-induced obesity in mice. Am. J. Physiol. Cell Physiol. *291*, C1232–C1239.

Chan, C.W., Crafton, E., Fan, H.N., Flook, J., Yoshimura, K., Skarica, M., Brockstedt, D., Dubensky, T.W., Stins, M.F., Lanier, L.L., et al. (2006). Interferon-producing killer dendritic cells provide a link between innate and adaptive immunity. Nat. Med. *12*, 207–213.

Chawla, A., Nguyen, K.D., and Goh, Y.P. (2011). Macrophage-mediated inflammation in metabolic disease. Nat. Rev. Immunol. *11*, 738–749.

Cildir, G., Akıncılar, S.C., and Tergaonkar, V. (2013). Chronic adipose tissue inflammation: all immune cells on the stage. Trends Mol. Med. *19*, 487–500.

De Souza, C.T., Araujo, E.P., Bordin, S., Ashimine, R., Zollner, R.L., Boschero, A.C., Saad, M.J., and Velloso, L.A. (2005). Consumption of a fat-rich diet activates a proinflammatory response and induces insulin resistance in the hypothalamus. Endocrinology *146*, 4192–4199.

Dhodapkar, M.V., Steinman, R.M., Krasovsky, J., Munz, C., and Bhardwaj, N. (2001). Antigen-specific inhibition of effector T cell function in humans after injection of immature dendritic cells. J. Exp. Med. *193*, 233–238.

Elgazar-Carmon, V., Rudich, A., Hadad, N., and Levy, R. (2008). Neutrophils transiently infiltrate intra-abdominal fat early in the course of high-fat feeding. J. Lipid Res. *49*, 1894–1903.

Eller, K., Kirsch, A., Wolf, A.M., Sopper, S., Tagwerker, A., Stanzl, U., Wolf, D., Patsch, W., Rosenkranz, A.R., and Eller, P. (2011). Potential role of regulatory T cells in reversing obesity-linked insulin resistance and diabetic nephropathy. Diabetes *60*, 2954–2962.

Feuerer, M., Herrero, L., Cipolletta, D., Naaz, A., Wong, J., Nayer, A., Lee, J., Goldfine, A.B., Benoist, C., Shoelson, S., and Mathis, D. (2009). Lean, but not obese, fat is enriched for a unique population of regulatory T cells that affect metabolic parameters. Nat. Med. *15*, 930–939.

Fu, F., Li, Y., Qian, S., Lu, L., Chambers, F., Starzl, T.E., Fung, J.J., and Thomson, A.W. (1996). Costimulatory molecule-deficient dendritic cell progenitors (MHC class II+, CD80dim, CD86-) prolong cardiac allograft survival in nonimmunosuppressed recipients. Transplantation *62*, 659–665.

Guilherme, A., Virbasius, J.V., Puri, V., and Czech, M.P. (2008). Adipocyte dysfunctions linking obesity to insulin resistance and type 2 diabetes. Nat. Rev. Mol. Cell Biol. *9*, 367–377.

Hotamisligil, G.S., Shargill, N.S., and Spiegelman, B.M. (1993). Adipose expression of tumor necrosis factor-alpha: direct role in obesity-linked insulin resistance. Science *259*, 87–91.

Ilan, Y., Maron, R., Tukpah, A.M., Maioli, T.U., Murugaiyan, G., Yang, K., Wu, H.Y., and Weiner, H.L. (2010). Induction of regulatory T cells decreases adipose inflammation and alleviates insulin resistance in ob/ob mice. Proc. Natl. Acad. Sci. USA *107*, 9765–9770.

Jonuleit, H., Schmitt, E., Schuler, G., Knop, J., and Enk, A.H. (2000). Induction of interleukin 10-producing, nonproliferating CD4(+) T cells with regulatory properties by repetitive stimulation with allogeneic immature human dendritic cells. J. Exp. Med. *192*, 1213–1222.

Kägi, D., Ledermann, B., Bürki, K., Seiler, P., Odermatt, B., Olsen, K.J., Podack, E.R., Zinkernagel, R.M., and Hengartner, H. (1994). Cytotoxicity mediated by T cells and natural killer cells is greatly impaired in perforin-deficient mice. Nature *369*, 31–37.

Kang, K., Reilly, S.M., Karabacak, V., Gangl, M.R., Fitzgerald, K., Hatano, B., and Lee, C.H. (2008). Adipocyte-derived Th2 cytokines and myeloid PPARdelta regulate macrophage polarization and insulin sensitivity. Cell Metab. *7*, 485–495.

Liu, J., Divoux, A., Sun, J., Zhang, J., Clément, K., Glickman, J.N., Sukhova, G.K., Wolters, P.J., Du, J., Gorgun, C.Z., et al. (2009). Genetic deficiency and pharmacological stabilization of mast cells reduce diet-induced obesity and diabetes in mice. Nat. Med. *15*, 940–945.

Lu, L., Qian, S., Hershberger, P.A., Rudert, W.A., Lynch, D.H., and Thomson, A.W. (1997). Fas ligand (CD95L) and B7 expression on dendritic cells provide counter-regulatory signals for T cell survival and proliferation. J. Immunol. *158*, 5676–5684.

Lumeng, C.N., Bodzin, J.L., and Saltiel, A.R. (2007a). Obesity induces a phenotypic switch in adipose tissue macrophage polarization. J. Clin. Invest. *117*, 175–184.

Lumeng, C.N., Deyoung, S.M., Bodzin, J.L., and Saltiel, A.R. (2007b). Increased inflammatory properties of adipose tissue macrophages recruited during diet-induced obesity. Diabetes *56*, 16–23.

Lutz, M.B., Kukutsch, N.A., Menges, M., Rössner, S., and Schuler, G. (2000). Culture of bone marrow cells in GM-CSF plus high doses of lipopolysaccharide generates exclusively immature dendritic cells which induce alloantigen-specific CD4 T cell anergy in vitro. Eur. J. Immunol. *30*, 1048–1052.

Ndifon, W., Gal, H., Shifrut, E., Aharoni, R., Yissachar, N., Waysbort, N., Reich-Zeliger, S., Arnon, R., and Friedman, N. (2012). Chromatin conformation governs T-cell receptor Jβ gene segment usage. Proc. Natl. Acad. Sci. USA *109*, 15865–15870.

Nguyen, M.T.A., Favelyukis, S., Nguyen, A.K., Reichart, D., Scott, P.A., Jenn, A., Liu-Bryan, R., Glass, C.K., Neels, J.G., and Olefsky, J.M. (2007). A subpopulation of macrophages infiltrates hypertrophic adipose tissue and is activated by free fatty acids via Toll-like receptors 2 and 4 and JNK-dependent pathways. J. Biol. Chem. *282*, 35279–35292.

Nishimura, S., Manabe, I., Nagasaki, M., Eto, K., Yamashita, H., Ohsugi, M., Otsu, M., Hara, K., Ueki, K., Sugiura, S., et al. (2009). CD8+ effector T cells contribute to macrophage recruitment and adipose tissue inflammation in obesity. Nat. Med. *15*, 914–920.

Nishimura, S., Manabe, I., Takaki, S., Nagasaki, M., Otsu, M., Yamashita, H., Sugita, J., Yoshimura, K., Eto, K., Komuro, I., et al. (2013). Adipose natural regulatory B cells negatively control adipose tissue inflammation. Cell Metab., S1550-4131(13)00386-0.

Odegaard, J.I., Ricardo-Gonzalez, R.R., Goforth, M.H., Morel, C.R., Subramanian, V., Mukundan, L., Red Eagle, A., Vats, D., Brombacher, F., Ferrante, A.W., and Chawla, A. (2007). Macrophage-specific PPARgamma controls alternative activation and improves insulin resistance. Nature *447*, 1116–1120.

Osborn, O., and Olefsky, J.M. (2012). The cellular and signaling networks linking the immune system and metabolism in disease. Nat. Med. *18*, 363–374.

Ouchi, N., Parker, J.L., Lugus, J.J., and Walsh, K. (2011). Adipokines in inflammation and metabolic disease. Nat. Rev. Immunol. *11*, 85–97.

Pillarisetty, V.G., Katz, S.C., Bleier, J.I., Shah, A.B., and Dematteo, R.P. (2005). Natural killer dendritic cells have both antigen presenting and lytic function and in response to CpG produce IFN-γ via autocrine IL-12. J. Immunol. *174*, 2612–2618.

Rausch, M.E., Weisberg, S., Vardhana, P., and Tortoriello, D.V. (2008). Obesity in C57BL/6J mice is characterized by adipose tissue hypoxia and cytotoxic T-cell infiltration. Int. J. Obes. *32*, 451–463.

Revelo, X.S., Tsai, S., Lei, H., Luck, H., Ghazarian, M., Tsui, H., Shi, S.Y., Schroer, S., Luk, C.T., Lin, G.H., et al. (2015). Perforin is a novel immune regulator of obesity-related insulin resistance. Diabetes *64*, 90–103.

Rocha, V.Z., Folco, E.J., Sukhova, G., Shimizu, K., Gotsman, I., Vernon, A.H., and Libby, P. (2008). Interferon-gamma, a Th1 cytokine, regulates fat inflammation: a role for adaptive immunity in obesity. Circ. Res. *103*, 467–476.

Sadyś, M., Strzelczak, A., Grinn-Gofroń, A., and Kennedy, R. (2015). Application of redundancy analysis for aerobiological data. Int. J. Biometeorol. *59*, 25–36.

Sakaguchi, S. (2000). Regulatory T cells: key controllers of immunologic self-tolerance. Cell *101*, 455–458.

Schipper, H.S., Prakken, B., Kalkhoven, E., and Boes, M. (2012). Adipose tissue-resident immune cells: key players in immunometabolism. Trends Endocrinol. Metab. *23*, 407–415.

Stary, G., Bangert, C., Tauber, M., Strohal, R., Kopp, T., and Stingl, G. (2007). Tumoricidal activity of TLR7/8-activated inflammatory dendritic cells. J. Exp. Med. *204*, 1441–1451.

Sun, K., Kusminski, C.M., and Scherer, P.E. (2011). Adipose tissue remodeling and obesity. J. Clin. Invest. *121*, 2094–2101.

Süss, G., and Shortman, K. (1996). A subclass of dendritic cells kills CD4 T cells via Fas/Fas-ligand-induced apoptosis. J. Exp. Med. *183*, 1789–1796.

Taieb, J., Chaput, N., Ménard, C., Apetoh, L., Ullrich, E., Bonmort, M., Péquignot, M., Casares, N., Terme, M., Flament, C., et al. (2006). A novel dendritic cell subset involved in tumor immunosurveillance. Nat. Med. *12*, 214–219.

Talukdar, S., Oh, Y., Bandyopadhyay, G., Li, D., Xu, J., McNelis, J., Lu, M., Li, P., Yan, Q., Zhu, Y., et al. (2012). Neutrophils mediate insulin resistance in mice fed a high-fat diet through secreted elastase. Nat. Med. *18*, 1407–1412.

Tiao, M.M., Lu, L., Tao, R., Wang, L., Fung, J.J., and Qian, S. (2005). Prolongation of cardiac allograft survival by systemic administration of immature recipient dendritic cells deficient in NF-kappaB activity. Ann. Surg. *241*, 497–505.

Trinité, B., Chauvin, C., Pêche, H., Voisine, C., Heslan, M., and Josien, R. (2005). Immature CD4- CD103+ rat dendritic cells induce rapid caspase-independent apoptosis-like cell death in various tumor and nontumor cells and phagocytose their victims. J. Immunol. *175*, 2408–2417.

Vosshenrich, C.A.J., Lesjean-Pottier, S., Hasan, M., Richard-Le Goff, O., Corcuff, E., Mandelboim, O., and Di Santo, J.P. (2007). CD11cloB220+ interferon-producing killer dendritic cells are activated natural killer cells. J. Exp. Med. *204*, 2569–2578.

Waithman, J., Allan, R.S., Kosaka, H., Azukizawa, H., Shortman, K., Lutz, M.B., Heath, W.R., Carbone, F.R., and Belz, G.T. (2007). Skin-derived dendritic cells can mediate deletional tolerance of class I-restricted self-reactive T cells. J. Immunol. *179*, 4535–4541.

Weisberg, S.P., McCann, D., Desai, M., Rosenbaum, M., Leibel, R.L., and Ferrante, A.W., Jr. (2003). Obesity is associated with macrophage accumulation in adipose tissue. J. Clin. Invest. *112*, 1796–1808.

Winer, S., Chan, Y., Paltser, G., Truong, D., Tsui, H., Bahrami, J., Dorfman, R., Wang, Y., Zielenski, J., Mastronardi, F., et al. (2009). Normalization of obesity-associated insulin resistance through immunotherapy. Nat. Med. *15*, 921–929.

Wu, D., Molofsky, A.B., Liang, H.E., Ricardo-Gonzalez, R.R., Jouihan, H.A., Bando, J.K., Chawla, A., and Locksley, R.M. (2011). Eosinophils sustain adipose alternatively activated macrophages associated with glucose homeostasis. Science *332*, 243–247.

Xu, H., Barnes, G.T., Yang, Q., Tan, G., Yang, D., Chou, C.J., Sole, J., Nichols, A., Ross, J.S., Tartaglia, L.A., and Chen, H. (2003). Chronic inflammation in fat

plays a crucial role in the development of obesity-related insulin resistance. J. Clin. Invest. *112*, 1821–1830.

Yang, H., Youm, Y.H., Vandanmagsar, B., Ravussin, A., Gimble, J.M., Greenway, F., Stephens, J.M., Mynatt, R.L., and Dixit, V.D. (2010). Obesity increases the production of proinflammatory mediators from adipose tissue T cells and compromises TCR repertoire diversity: implications for systemic inflammation and insulin resistance. J. Immunol. *185*, 1836–1845.

Yeung, K.Y., and Ruzzo, W.L. (2001). Principal component analysis for clustering gene expression data. Bioinformatics *17*, 763–774.

Yu, P., Xiong, S., He, Q., Chu, Y., Lu, C., Ramlogan, C.A., and Steel, J.C. (2009). Induction of allogeneic mixed chimerism by immature dendritic cells and bone marrow transplantation leads to prolonged tolerance to major histocompatibility complex disparate allografts. Immunology *127*, 500–511.

Zangi, L., Klionsky, Y.Z., Yarimi, L., Bachar-Lustig, E., Eidelstein, Y., Shezen, E., Hagin, D., Ito, Y., Takai, T., Reich-Zeliger, S., et al. (2012). Deletion of cognate CD8 T cells by immature dendritic cells: a novel role for perforin, granzyme A, TREM-1, and TLR7. Blood *120*, 1647–1657.